Task 3. Catalyst Characterization

The objective of this task is to obtain characterization data of the prepared catalysts using routine and selected techniques.

A. Characterization of Pt-Re Promoted Co/Al_2O_3 Catalysts

Introduction

We are continuing to study the impact on reducibility of cobalt oxides by the use of different supports and by the incorporation of different promoters and additives to supported cobalt catalysts. The reduction of Co_3O_4, which is present on the catalyst after calcination, is a two step process which passes through an intermediate CoO phase before reduction to the metal. In our prevoius investigations, we found by temperature programmed reduction that a $15\%Co/Al_2O_3$ displayed a broad second peak attributed to the reduction of cobalt species interacting with the support. In agreement, hydrogen chemisorption with pulse reoxidation revealed that the unpromoted catalyst displayed poor percentage reduction of only 30% after reduction at 623K, the standard activation temperature of Co FTS catalysts. While promotion of supported Co catalysts with the noble metal promoters Pt and Ru had a similar effect on catalyzing both reduction steps of Co_3O_4 to Co metal, Re only aided in catalyzing the second step when a significant interaction of the Co species with the support was present, such as found on Al_2O_3 supported catalysts. After reduction at 623K, therefore, the number of Co active sites increases remarkably with the addition of noble metal promoter, thereby increasing the initial activity under reaction testing.

We have investigated the possibility of a synergism between Pt and Re on the reducibility of supported Co oxides, and are testing the catalysts in the CSTR to draw conclusions as to the effect of Pt-Re promotion and synergism on the catalyst stability.

Catalyst Preparation

Condea Vista Catalox B γ-alumina (100-200 mesh, 200 m^2/g, pore volume 0.4 cm^3/g) was used as support material for the preparation of 15% loaded cobalt FTS catalysts. A three-step incipient wetness impregnation method was used to add 15 wt % cobalt to the supports with a drying procedure at 353K in a rotary evaporator following each impregnation. Noble metal promoted catalysts were prepared with different loadings of platinum and/or rhenium after cobalt addition and prior to calcination. Where both promoters were added, the Pt was loaded first. Catalysts were calcined only one time in air at 673K for 4hrs following the final impregnation step.

Catalyst Characterization

BET Surface Area

BET measurements were conducted using a Micromeritics Tri-Star system for all catalysts to determine the loss of surface area, if any, following loading of the metal. Prior to testing, samples were slowly ramped to 433K and evacuated for 4hrs to approximately 50mTorr.

Temperature Programmed Reduction

Temperature programmed reduction (TPR) profiles of catalysts were recorded using a Zeton Altamira AMI-200 unit. Calcined fresh samples were first purged in flowing inert gas at 623K to remove traces of water. TPR was performed using a 10%H_2/Ar mixture referenced to Ar at a flowrate of 30 ccm. The sample was heated from 323K to 1073K using a heating ramp of 10K/min and the H_2 consumption measured using a thermal conductivity detector (TCD)..

H_2 Chemisorption by TPD and % Reducibility by Pulse Reoxidation

The amount of chemisorbed hydrogen was measured using the Zeton Altamira AMI-200 unit. The sample weight was always 0.220 g. The catalyst was activated using hydrogen at 623K for 10hrs and cooled under flowing hydrogen to 373K. The sample was held at 373K under flowing argon to prevent adsorption of physisorbed and weakly bound species, prior to

increasing the temperature slowly to the activation temperature. At that temperature, the catalyst was held under flowing argon to desorb the remaining chemisorbed hydrogen until the TCD signal returned to the baseline. The TPD spectrum was integrated and the number of moles of desorbed hydrogen determined by comparing to the areas of calibration pulses of hydrogen in argon. Prior to experiments, the sample loop was calibrated with pulses of N_2 in a helium flow and compared against a calibration line produced from using gas tight syringe injections of N_2 into a helium flow. The volume of the loop was found to be 52 μL.

After TPD of H_2, the sample was reoxidized at 623K by pulses of pure O_2 in helium carrier referenced to helium gas. After oxidation of the cobalt metal clusters (where the entire O_2 pulse was observed by the TCD), the number of moles of O_2 consumed was determined, and the percent reducibility was calculated assuming that Co^0 reoxidized to Co_3O_4.

Diffuse Reflectance Infrared Fourier Transform Spectroscopy (DRIFTS) of adsorbed CO

Infrared spectroscopy of adsorbed CO was performed on a Nicolet Nexus 870 FT-IR which is equipped with a DTGS detector. The catalyst was mixed with KBr and placed into a Spectra-Tech High Temperature/High Pressure DRIFTS cell with ZnSe windows that allowed us to perform in situ thermal pretreatments. For each IR spectrum, taken at a resolution of 8 cm^{-1}, 128 scans were added. Samples were pre-reduced ex-situ under H_2:He (2:1) flow of 100 ccm/g catalyst at 623 K and passivated with 1%O_2 in helium at room temperature for 24 hours. Prior to each spectrum, the catalyst was re-reduced in situ in a flow of 33%H_2 in helium for one hour, held in helium for 30 minuted and cooled under helium flow (note: oxygen scrubbers were employed) to room temperature. The background was recorded at this time. Then, the catalyst was exposed to 1%CO in helium for 30 minutes at room temperature, scanned, purged in helium for 30 minutes, and scanned again. The latter step was employed to remove the contributions of gas phase and weakly adsorbed CO.

Results and Discussion

Results of surface area measurements by physisorption of nitrogen are reported in Table 1. Results show that the BET surface area for the 15% loaded Co catalysts on 200 m^2/g γ-Al_2O_3 were all close to 160 m^2/g. A weight % loading of 15% metal is equivalent to 20% by weight Co_3O_4. If the Al_2O_3 is the main contributor to the area, then the area of the Co/Al_2O_3 catalysts should be 0.80 ×200 m^2/g = 160 m^2/g, which matches the measured value. As shown in Table 1, addition of small quantities of noble metal promoters did not measurably impact the BET area.

Figure 1 shows the results of TPR. The unpromoted catalyst exhibits two peaks, and remarkably, the second peak is much broader than observed for similarly loaded TiO_2 and SiO_2 supported Co catalysts. Note that in the TPR, we did not ramp the temperature high enough to observe the reduction of bulk cobalt aluminate species, which has been shown to occur above 1073 K with up to 30% loading of cobalt. Therefore, the broad peak on the unpromoted catalyst (ca. 700 to 1000 K) is attributed to the reduction of Co surface species interacting with the support, and the different shoulders are likely due to varying degrees of interaction with the support as a function of cluster size. The smallest Co surface species, with the greatest interaction with the support, are therefore likely represented by the 950 K shoulder. The precise identity of these species is not clear, although it is surmised that the species are either the result of a strong interaction between very small cobalt oxide clusters and the support (deviating from bulklike cobalt oxides and reducing at higher temperatures than the bulk oxides) or small surface Co species which include support atoms in the structure (reducing at temperatures below that of bulk Co-aluminate). Hereafter, the species responsible for this peak will be referred to loosely as "Co surface support species". The addition of 0.5%Pt caused the peaks to shift markedly to lower temperatures, presumably due to spillover of H_2 from the metallic promoter to reduce the Co oxide and Co surface support species.

The reduction of Re oxide occurs at higher temperatures than Pt oxide. Figure 1 shows that although there appears to be no improvement in the reduction of the low temperature peak

assigned to the reduction of cobalt oxides, Re still plays a valuable role in decreasing the reduction temperature of Co species for which there is a significant surface interaction with the support. Our previous work shows that Re oxide reduces at 620K, which may explain the lack of effect on the low temperature peak responsible for reduction of cobalt oxides. TPR profiles in Figure 1 show that bulk cobalt oxide has essentially been reduced before the Re oxide is reduced, so no spillover effect can operate to aid in reducing those species. However, H_2 spillover from the reduced Re metal occurs to facilitate reduction of Co species interacting with the support only after the reduction peak of Re oxide to Re metal is achieved.

By keeping the same number of moles of noble metal promoter but by varying the ratio of Pt and Re, interesting effects on reduction are observed in TPR. The best molar ratio appears to be 50%Pt and 50%Re. Relative to Pt promoted catalyst, the addition of Re appears to sharpen the peaks somewhat, while relative to Re, both peaks are shifted to lower temperatures. Since our preliminary findings show that Re promotion results in a more stable catalyst than Pt promotion of Co/Al_2O_3, addition of Pt to a Re-promoted catalyst may aid in catalyzing Re reduction.

Results of H_2 chemisorption by TPD (Table 2) after reduction at 623K indicate that the number of surface sites increases with addition of either Pt or Re promoter. By performing pulse reoxidation, it is clear that the remarkable gain in Co^0 site density is mainly due to an enhancement in the reducibility of the clusters, and not to improvements in the actual dispersion (cluster size) of the reduced cobalt. Addition of Pt or Re causes a fraction of the smaller Co surface species that interact with the support to be reduced in this temperature range. Results of H_2 chemisorption by TPD and pulse reoxidation (Table 2) revealed that, for both unpromoted and promoted catalysts, there were significant increases (from 30% to approximately 60% with addition of 0.5% noble metal promoter). Maintaining the 50%Pt/50%Re molar ratio but

doubling the loading increased the percentage further to 72%. This is in line with the further observed shifts of both peaks in the TPR.

DRIFTS of adsorbed CO is useful for probing the electronic and geometric effects of promoters on supported metal catalysts. Figure 2 shows the resulting spectra after purging the gas phase and weakly bound species with helium at room temperature. The linear stretch vibration of CO adsorbed on Co occurs at approximately 1980 cm^{-1}, while the bridged species are observed at lower wavenumbers. An interesting trend emerges where increasing Re concentration results in a decrease in the linear to bridge-bonded CO ratio (Table 3). Typically, an increase in bridge bonded CO is the result of larger clusters present on the catalyst. The possibility also exists that the increase in linear bonded CO for the Pt promoted catalyst may be the result of a geometric alloying effect, whereby Pt might break up the geometry to Co sites. Clearly, adsorption of CO also occurs on the promoter. For CO on Pt, the band occurs at approximately 2080 cm^{-1}. However, one cannot rule out the possibility of an electronic effect.

To test for the possibility of alloy formation, we are continuing to study these catalysts by High Resolution Transmission Electron Microscopy. With this technique, we may be able to determine if there are changes in the lattice spacing due to alloy formation. At this time, important differences were observed for Pt and Re promoted catalysts in terms of reducibility and catalyst stability. Future catalytic testing results combined with characterization should provide insight into the nature of these differences.

Table 1

BET surface areas

Support/Catalyst	BET SA (m^2/g)	Ave Pore Size (nm)	Calcination T (K)
Condea Vista Catalox B γ-Al_2O_3	200	-	-
Unpromoted 15%Co/ γ-Al_2O_3	161.5	4.14	623, flow
0.5%Pt/15%Co/Al_2O_3	156.1	3.97	623, flow
0.477%Re/15%Co/Al_2O_3	160.2	3.94	623, flow
0.239%Re/0.25%Pt/15%Co/Al_2O_3	157.7	4.01	623, flow
0.477%Re/0.5%Pt/15%Co/Al_2O_3	160.5	3.92	623, flow
0.358%Re/0.125%Pt/15%Co/Al_2O_3	166.5	3.92	623, flow
0.120%Re/0.375%Pt/15%Co/Al_2O_3	161.5	3.96	623, flow

Table 2

H_2 Chemisorption by TPD and Percentage Reduction by Pulse Reoxidation

Sample Description	Red T(K)	Micromoles H_2-Desorbed/g	Uncorr. Disp.	Uncorr. Diam. (nm)	% Reduced	Corr. Diam. (nm)	Corr. Dispersion
Unpromoted 15% Co/Al_2O_3	623	70.5	5.5%	18.6	29%	5.4	19.1%
with 0.5% Pt	623	151	11.9%	8.7	64%	5.6	18.6%
with 0.120% Re/0.375% Pt	623	148.6	11.7%	7.7	61%	5.4	19.2%
with 0.239% Re/0.25% Pt	623	157.7	12.4%	7.3	63%	5.2	19.7%
with 0.358% Re/0.125% Pt	623	139.7	11.0%	9.5	61%	5.7	18.0%
with 0.477% Re	623	136.7	10.7%	9.6	65%	6.2	16.5%
with 0.477% Re/0.5% Pt	623	175.5	13.8%	7.5	72%	5.4	19.2%

Table 3

Linear to Bridged Ratio for Adsorbed CO as Measured by DRIFTS

Catalyst	L/B
15% Co/AL_2O_3	0.296
0.5% Pt-15% Co/Al_2O_3	0.258
0.375% Pt-0.20% Re-15% Co/Al_2O_3	0.308
0.235% Re-0.25% Pt-15% Co/Al_2O_3	0.269
0.477% Re-0.5% Pt-15% Co/Al_2O_3	0.242
0.36% Re-0.125% Pt-15% Co/Al_2O_3	0.207
0.477% Re-15% Co/Al_2O_3	0.195

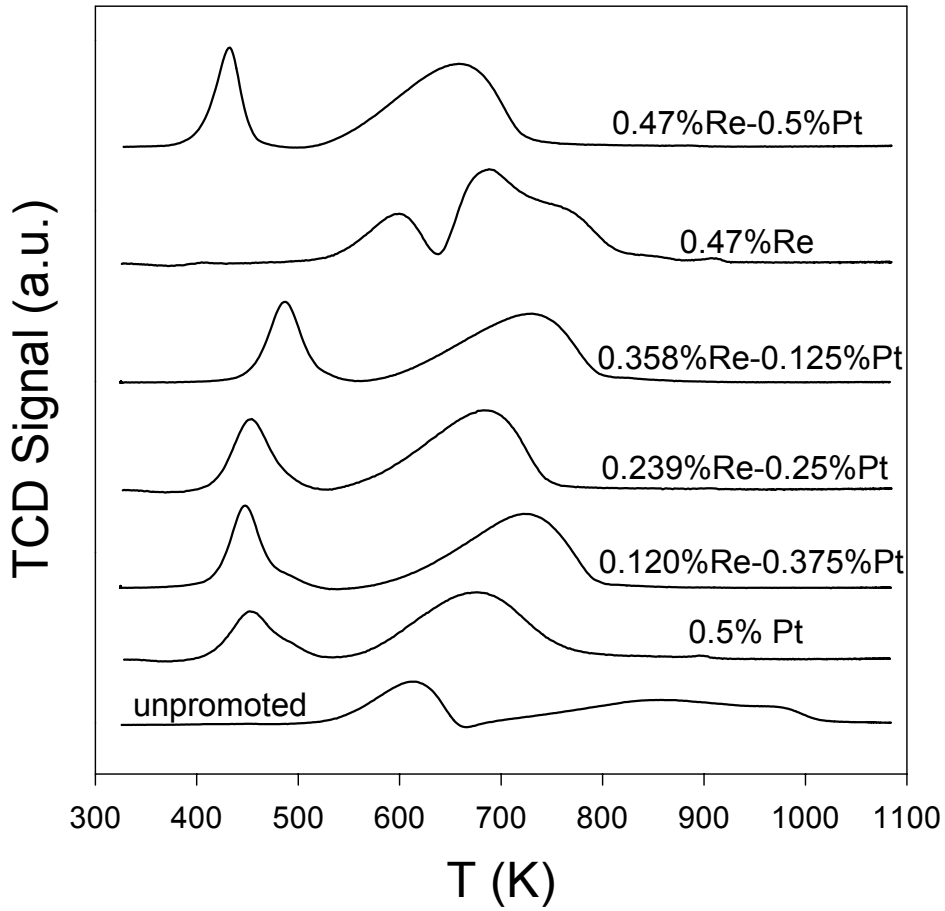

Figure 1. TPR profiles of Pt and/or Re promoted 15% Co/Al_2O_3 catalysts.

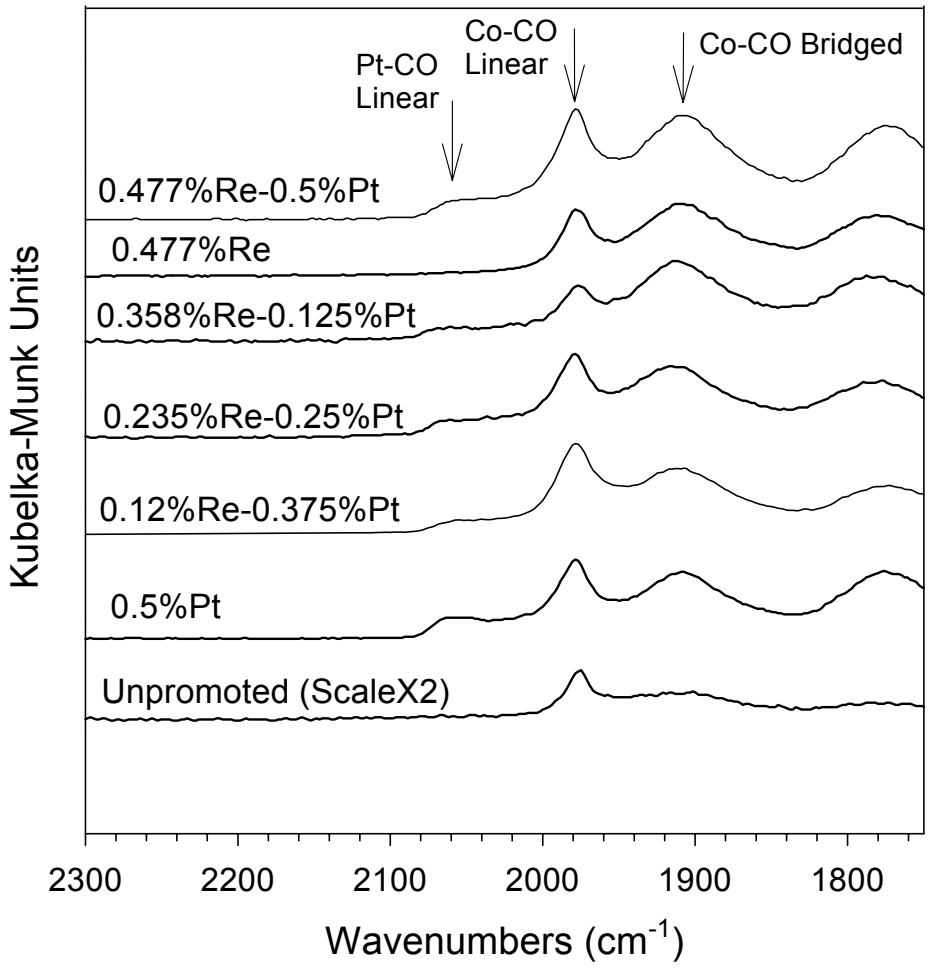

Figure 2. DRIFTS of adsorbed CO profiles of Pt and/or Re promoted 15% Co/Al_2O_3 catalysts.

Task 4. Wax/Catalyst Separation

The objective of this task is to develop techniques for the separation of catalysts from FT reactor slurries.

A. Slurry Bubble Column Reactor (SBCR) Activities

Executive Summary

In this report we describe SBCR pilot plant results and operating experiences using an improved catalyst/slurry filtration system. The following improvements to the filtration system were included: an enlarged let-down valve trim, an automatic differential pressure controller for the filter media and a by-pass for the let-down valve. Further filtration tests were conducted using a high alpha iron-based F-T catalyst. During the activation, problems were encountered with the gas sparger in several pilot runs. Catalyst had infiltrated the sintered metal sparger causing an excessive pressure drop. A new activation procedure was developed to minimize sparger plugging.

As in previous reported pilot-scale experiments, conversion results of the high alpha catalyst in the SBCR were compared to that of CSTR experiments. A method for estimating the SBCR recirculation rate is also described.

Introduction

A Slurry Bubble Column Reactor (SBCR) is a gas-liquid-solid reactor in which the finely divided solid catalyst is suspended in the liquid by the rising gas bubbles. Fischer-Tropsch Synthesis (FTS) takes place in a SBCR where the synthesis gas is converted on catalysts suspended as fine particles in a liquid. The synthesis gas flows in a bubble phase through the catalyst/wax suspension. The bubbles in the catalyst slurry are produced by a gas distributor or sparger in the bottom of the reactor. The volatile products are removed with unconverted gases, and the liquid products are separated from the suspension.

<u>Separation of Wax Products From Catalysts</u>

Heavy wax products must be separated from catalyst particles before being removed from the reactor system. Achieving an efficient wax product separation from the catalyst is one of the most challenging technical problems associated with slurry-phase F-T. A number of processes have been proposed to separate heavy wax liquids from a catalyst slurry in BCRs. Brennan [1] patented a process for removing catalyst fines from a wax slurry using a magnetic separator. Catalyst fines are held by a magnetized filter element while the wax passes unabated. Two external pumps are used in the system, one pump extracts a portion of the reactor slurry while another pump returns the captured catalyst particles to the BCR.

Lorentzen [2] developed and patented a process in which liquid products are separated from a slurry phase containing catalyst particles using a series of vertical reaction tubes in parallel. A separate filter member ring is provided near the top of each tube. The filtrate from each ring overflowed into a weir and centrally collected for further processing. Several configurations of the filtration zone are described in detail.

Sasol [3] patented an internal filtration system for F-T BCRs. Their invention consists of a plurality of wire mesh filter units connected in parallel within the BCR vessel. Critical parameters such as filtration and back-flushing rates per unit area of filter are detailed. This system has the advantage of minimizing the hold-up of catalyst slurry outside the reactor vessel. However, internal systems are difficult if or sometimes impractical to service without taking the reactor vessel off-line.

A cross-flow filtration invention is outlined in a U.S. Patent by Engel, et al [4]. Their system extracts gas and catalyst slurry from a BCR column via an external pump. The slurry is degassed by a hydroclone and is directed to a cross-flow inertial filter. A slurry velocity of 1 to 6 m/s must be maintained for efficient filter operation. The system has the disadvantage of requiring an external pump that could accelerate catalyst attrition.

Benham [5] developed a separation system that includes a dynamic settling device placed within a natural convection recirculation loop. Slurry flows through an external downcomer into a nozzle positioned within an expansion chamber. Heavy and large particles exit the bottom of the chamber and continue through a downcomer loop into the bottom of the slurry bubble column. Near the top of the expansion chamber in an annulus section, a stream containing diluted slurry is extracted for further filtration. One embodiment of the invention places the separation chamber inside the BCR.

Robert [6] has developed a method of extracting a Fischer-Tropsch catalyst from the output slurry of a Fischer-Tropsch bubble column reactor that involves contacting extracted slurry with a supercritical hydrocarbon solvent. F-T products are recovered in a 2-stage extraction process. The disadvantage with this system is that many vessels are required outside the BCR, thus requiring a considerable hold-up of catalyst outside the system.

Filtration Study Objective

As discussed in the previous reports [7,8,9], the CAER 5.08 cm diameter SBCR plant was overhauled and redesigned to incorporate automatic slurry level control and wax filtration systems. The wax filtration system was designed to accept a variety of filter elements. These additions enhance the stability of the reactor for long-term tests useful for both catalyst deactivation and attrition studies under SBCR synthesis conditions.

In the following discussion, we will detail the results and operational experiences of an experimental SBCR run using a high-alpha, precipitated/spray-dried iron catalysts. Objective of the run was to test the effectiveness of modifications to the wax filtration system. The FTS data obtained from the SBCR system were to be compared with a similar CSTR run.

Experimental

The SBCR apparatus, shown in Figure 1, was originally designed as a direct coal liquefaction reactor. In the current configuration, the bubble column has a 5.08 cm diameter and

a 2-m height with an effective reactor volume of 3.7 liters. The synthesis gas was passed continuously through the reactor and distributed by a sparger near the bottom of the reactor vessel. The product gases and slurry exit the top of the reactor and pass through an overhead receiver vessel where the slurry was disengaged from the gas-phase. Vapor products and unreacted syngas exit the overhead vessel, enter a warm trap (100 ^{o}C), and a cold trap (3^{o}C). A dry flow meter down stream of the cold trap was used to measure the exit gas flow rate.

A dip tube was added to the reactor vessel so that the F-T catalyst slurry could be recycled internally via a natural convection loop. The unreacted syngas, F-T products, and slurry exited into a side port near the top of the reactor vessel and entered a riser tube. The driving force for the recirculation flow was essentially the difference in density between the fluid column in the riser (slurry and gas) and that of the dip-tube (slurry only). The dip tube provided a downward flow path for the slurry without interfering with the upward flow of the turbulent syngas slurry mixture. Thus, to some degree, back mixing of the slurry phase and wall effects in the narrow reactor tube were minimized.

Catalyst Activation and SBCR Startup Procedure. Periodically, an excessive pressure drop across the gas sparger has occurred during the activation portion of the pilot runs. Most likely, catalyst infiltrates into the sintered metal matrix during catalyst loading. The hydrostatic pressure from the catalyst and start-up oil in addition to argon pressure into the overhead vessel forced catalyst into the sparger. One pilot run had to be aborted as a result of this phenomenon. In order to correct this problem, the 1 mm Mott sparger was replaced with a more porous 20 mm sparger. Additionally, the activation procedure was modified such that gas flow was initiated through the sparger immediately after the catalyst had been loaded.

In preparation for catalyst activation, the SBCR was filled with 2.8 liters (~75% of the reactor volume) of a slurry consisting of 20 wt.% iron catalyst and Shell C_{30} oil. An additional 1.3 liters of the C_{30} oil was isolated in the overhead separation vessel. The reactor was

pressurized with flowing CO gas at 175 psig (12 atm) while the slurry temperature was increased to the desired activation temperature at a 50 ^{o}C/ hour rate. The valves in the down-comer line were opened to allow flow of the C30 in the overhead receiver to flow downward into the reactor. Thus, the recirculation between the reactor vessel and the overhead receiver was initiated. Once the reactor temperature stabilized, the exit gas was periodically monitored for CO_2 to observe the progress of activation. After the catalyst had been activated (~36 hours), hydrogen gas flow was phased in with the CO feed gas. Once the reactor temperatures had stabilized, CO, H_2, and syngas conversions were calculated at least once a day to monitor the reactor performance.

Wax Filtration Equipment and Procedure. For the current study, a cross-flow filter tube from Mott Metallurgical Corporation (Model # 7610- ½ - 5 - AB) was installed in the liquid down-comer tube below the overhead separation vessel. A detailed schematic of the filtration system is shown in Figure 2. The filter unit is a flow-through device having a sintered metal (5 mm average pore size) tube in a shell. Filtered wax was extracted radially through the tube while slurry flows downward in the axial direction (as shown in Figure 3). Ideally, the effectiveness of this type of filter depends on the inertia of the solid particles in the axial direction. Mott specifies that the axial velocity should be greater than 6 m/s to minimize particle migration toward the sintered filter media in the radial direction.

Filtered wax was metered into a storage tank through a letdown valve operated by the overhead liquid level controller. Pressure drop across the filter media was controlled automatically by a back-pressure regulator in the wax storage tank pressure. The filter assembly was configured such that the filter media could be replaced on-line, without aborting or interrupting the reactor run. A by-pass line was installed around the let-down valve to used in the event of a blockage in the control valve circuit.

The level or volume of the slurry within the receiver was continuously monitored by measuring the differential pressure across the height of the vessel. Argon was purged through each of the pressure legs to keep the lines free of slurry. Slurry volume within the receiver was controlled to be no more than 1.3 liters by removing wax from the reactor system via the level control valve. The unfiltered slurry flowed back to the reactor via a natural convection loop through a dip-tube exiting near the bottom of a reactor.

Discussion of Results

The run/activation conditions for the SBCR system along with the comparison CSTR run are listed in Table 1. A nominal space velocity of 5.0 slph/g was used for both reactor systems. The activation temperature for the SBCR and CSTR reactor tests was 270ºC. A high alpha iron-based, catalyst was prepared from a 75 kg batch of a precursor spray-dried catalyst having a composition of 100 Fe/4.4 Si/1.0 K. Approximately 750 g of the high alpha catalyst was prepared from the precursor by adding Cu and K promoters. The final composition of the high-alpha catalyst was 100 Fe/5.1 Si/2.0 Cu/ 5 K. This catalyst formulation was used in both the SBCR pilot unit (for filtration tests) and the 1 liter CSTR reactor under similar conditions in a continuing effort to quantify scale-up effects between the two reactor types.

SBCR Filtration System

Cross-Flow Filtration: Possible Mechanisms

The intended design of a cross-flow inertial filter system employs an inertial filter principle that allows the filtrate to flow radially through the porous media at a relatively low face velocity as compared to that of the mainstream slurry in the axial direction [10]. Catalyst entrained the high velocity axial flow are prevented from entering the porous media by the ballistic effect of particle inertia. Submicron particles penetrating the filter media, form a "dynamic membrane" or submicron layer as describe by the Mott Corporation as shown in Figure 4. The membrane impedes further penetration of even smaller particles through the porous filter media. This filtration mechanism is valid for an axial velocity greater than 6 m/s. Below this critical velocity, a filter cake of solids will form between the filter media and the bulk slurry flow and depicted in Figure 5. In this mode, multiple layers of catalyst particles deposit upon the filter medium acting as a pre-filter layer [11,12]. Both the inertial and filter-cake mechanisms can be effective; however, the latter can be unstable if the filter cake depth is allowed to grow indefinitely. In the context of the SBCR operation, the filter cake could potentially occlude the slurry recirculation flow path if allowed to grow uncontrollably. Therefore, if operating in the filter-cake mode, the axial velocity should be maintained at a level such that an adequate shear force exists along the filter media to prevent excessive caking of the catalyst that could cause a blockage in the down-comer circuit.

Estimation of the Down-Comer Slurry Velocity/Slurry Recirculation Rate

Quantifying the axial velocity in the cross-flow filter is a challenging problem. Since the driving force of the recirculation is quite small (the difference between the hydraulic head of the downcomer and that of the riser/reactor), any type of intrusive flow instrumentation could potentially alter the flow. However, by making a few simple assumptions, a method for

estimating of the recirculation rate and therefore the axial slurry velocity in the filter can be derived.

The rate of recirculation within the CAER's SBCR depends on the volumetric flow of the gas phase through the riser section between the reactor vessel and overhead vessel. Thus, at any given reactor pressure and catalyst concentration, the volumetric rate of gas flow is directly proportional to the space velocity. A simplified schematic of the recirculation process within the SBCR system is represented in Figure 6. Syngas enters the reactor vessel through the gas sparger and proceeds up the reactor with a gas hold-up fraction of ϵ_g. F-T product vapors and unreacted syngas exit the top of the reactor and enter the riser section at a rate denoted by Q_{Gas}. Slurry at the top of the reactor is entrained by the exit gas and proceeds in a slugging fashion up the narrow riser tube (Q_{LR}). Consequently, the riser section of the SBCR system functions as a gas-lift pump [13]. Slurry is disengaged from the gas phase in the overhead receiver and flows through the cross-flow filter unit at a rate Q_{LF}. A constant liquid level is maintained by extracting reactor wax product (Q_{LP}) . Since Q_{LP} is several orders of magnitude less than slurry rate exiting the filter (Q_{LF}) and the liquid level in the overhead receiver is constant, then we can assume that:

$$Q_{LF} \approx Q_{LR.} \tag{1}$$

If we assume the gas hold in the riser section is the same as that in the reactor, then by definition of gas hold, the following equation is valid at the riser:

$$\varepsilon_g \approx \frac{Q_{gas}}{Q_{gas} + Q_{LR}} \tag{2}$$

From online gas hold-up tests at reactor conditions (5 slph/g, P = 175 psi, and Ug = 3 cm/s), ϵ_g and Q_{gas} were experimentally determined to be 0.2 L L^{-1} and 1.8 actual L min^{-1}, respectively. Hence, Q_{LR} can be determined by rearranging equation (2):

$$Q_{LR} \approx \frac{Q_{Gas}(1-\varepsilon_g)}{\varepsilon_g} \approx 7\ lpm. \quad (3)$$

This liquid rate corresponds to an axial velocity of less than 1 m/s in the ½ inch I.D. filter element– well below the critical value of 6 m/s for inertial filtration. Therefore, the mode of filtration is likely the filter-cake method as shown in Figure 5.

Filter System Operation/Slurry Level Control

During the course of the pilot plant run for this study (Run #JKN-006), the reactor wax let-down line was used as a qualitative indicator for the rate of filtered wax removed from the reactor. The letdown line was heat-traced such that a nominal temperature of 90° C was maintained before filtration was initiated. When the slurry level controller opened the letdown valve, a temperature spike resulted from the influx of hot filtered wax (>200 °C). Therefore, higher filtration rates (when the letdown valve was opened) resulted in letdown temperatures increasingly above the 90° C baseline.

Initially, the differential pressure across the filter media was set to 55 psi, as specified by the manufacturer. Since the flow rate of filtered reactor wax is relatively small (typically less than 800 g/day), the level controller was set to be in the on/off mode. The letdown control valve trim was sized such that it's pressure loss was negligible; therefore, the pressure difference across the filter media was constant during filtration events.

The letdown line temperature and the slurry level are shown in Figure 7 for the time period near the beginning of the run when the filtration system was started. The first filter event is denoted by a temperature spike of about 130 °C (18:00 hrs, 6/22/01). The cycle time of the controller opening the letdown varied from 1 to 2 hours between letdown events. Once the valve was opened, the slurry level would drop approximately 0.15 to 0.30" below the set-point of 6.5" w.c. within a five minute period. This level drop corresponds to the programmed controller

dead-band. Once the dead-band level drop condition had been satisfied, the controller would close the letdown valve. After a day of the filter system being operational, the temperature spikes decreased in amplitude to less than 110 ^{o}C or only 20 ^{o} above the baseline temperature. This phenomenon is in all likelihood due to a filter-cake being established on the sintered metal media.

Continual fouling of the Mott filter was evident after about six days of filter operation or after 168 hours of TOS. The time the control valve remained open during each filter cycle steadily increased from five minutes (after the first letdown event) to being continuously open after 168 hours. The differential pressure across the filter media was set to 90 psi in an effort to increase the filtration flux with little success. After 168 hours TOS the slurry level increased to 1.5 " w.c. above the controller set-point, indicating that the filtered wax could not be removed at a rate sufficient to maintain a constant slurry level.

Future Filtration Procedures

Although the Mott filter performance declined after only 168 hours into the run, it had been in service in the previous two pilot runs without being removed for intensive cleaning. Normally, the filters are removed when a different catalyst is being tested or after 1000 hours of service. Hence, the filter had logged approximately 700 hours of in-service time. The used filters are subjected to cleaning in an ultrasonic bath for 48 hours and back-flushed with C_{30} oil. This maintenance procedure has been proven effective in dislodging submicron catalyst particles from the filter matrix.

During these earlier tests, the filter had been subjected to very high filtration fluxes and differential pressures while developing and refining operating procedures. The installation of a constant pressure controller on the filtrate side of the media improved the stability of the level control and will likely extend the service time of the Mott filter tube beyond 1000 hours. However, based on observations during run JKN-006, the starting differential pressure across the

filter media could be further decreased below the Mott-recommended 55 psi. This will cause the control valve to be open for longer periods thereby lowering the average filtration flux. This will decrease the degree of submicron particle infiltration into the sintered metal matrix of the filter tube. Consistently back-flushing of the filers with argon every 24 hours should also limit deep penetration of the particles into the filter.

High Alpha Catalyst Performance

Comparisons between CSTR and SBCR runs.

The gas conversions versus time-on-stream for the SBCR and CSTR systems are displayed in Figure 8. Hydrogen, CO, and syngas conversions in the SBCR reached a maximum after 96 hours time-on-stream (TOS). After this catalyst initiation period, the syngas conversion started to steadily decline to about 35% after 144 hours TOS. After 168 hours TOS the SBCR conversion started to decrease as a result of the level control/slurry filtration problems. The resulting slurry level increase effectively diluted the catalyst in the reactor and thereby increased the space velocity.

Maximum conversions in the CSTR were attained after 72 hours of TOS. Overall, the syngas conversions in the CSTR were consistently greater than that of the SBCR. This observation is inconsistent with the previously reported SBCR results [10]. SBCR conversions have been slightly higher than CSTR runs with similar operating conditions. We had attributed this behavior to the plug-flow nature of the SBCR reactor system. A portion of this anomaly can be explained by the SBCR space velocity being 9% higher than that of the CSTR.

F-T Product Distribution.

The averaged alpha plot distributions for the SBCR and CSTR high alpha experiments are displayed Figure 9. The durations of the runs were not sufficient to totally purge the system of the C_{30} startup oil, as evidenced by the protuberance in the alpha plot near n=28-32 in both the SBCR and CSTR plots. Similar single alpha values of 0.90 and 0.91 were calculated for the

SBCR and CSTR respectively. The weight percent distribution of light gas, gas, gasoline, diesel, and wax for both the CSTR and SBCR systems are listed in Table 2. The SBCR consistently produced less methane than the CSTR. Although the single alpha values were similar for the two reactor systems, the SBCR produced 68.0% C_{12}+ versus 60.0% in the CSTR. The alkene ratios for products up to carbon number 20 are quite similar for both reactor systems as shown in Figure 10.

Conclusions

A method for estimating slurry recirculation within the SBCR was developed. Axial velocity through the cross-flow filter, derived from the estimated slurry rate, was estimated to be less 6 m/s due to a low driving force of recirculation within the SBCR. Therefore, a filtration mechanism was proposed that is based on the formation of a filter-cake within the cross-flow tube.

A SBCR pilot plant run was successfully completed to test a new wax filtering procedure with a 5 mm filter media. The test was conducted using a high-alpha iron catalyst. An automatic differential pressure controller across the filter media allowed for a more consistent and stable reactor slurry level control. Further refinements to the filtration operation will include periodic back-flushing and using low differential pressures (less than 20 psi) across the filter media.

In contrast to previously reported results, pilot-scale SBCR gas conversions results were slightly lower than that of CSTR run under similar conditions. Overall FT alpha distributions and alkene ratios between the two reactor systems were quite similar.

NOMENCLATURE

P_F Filtrate pressure, PSI

P_{rxtr} Reactor pressure, PSI

Q_{Gas} Volumetric rate of gas exiting the reactor, $m^3\ s^{-1}$

Q_{LR} Volumetric rate of catalyst slurry exiting the reactor, $m^3\ s^{-1}$

Q_{LF} Volumetric rate of catalyst slurry exiting the cross-flow filter tube, $m^3\ s^{-1}$

Q_{LP} Volumetric rate of filtered reactor wax product, $m^3\ s^{-1}$

SV Gas space velocity, SL h^{-1} Fe·g^{-1}

TOS Time-on-stream, hours

U_g Superficial gas velocity based on inlet reactor conditions, cm s^{-1}

U_L Superficial liquid velocity, cm s^{-1}

w.c. Pressure in units of water column

X_{CO} CO conversion

ϵ_g Gas hold up fraction in the reactor vessel, L L^{-1}

ϵ_L Liquid hold up fraction in the reactor vessel, L L^{-1}

REFERENCES

1. Brennan, et al. , "Separation of Catalyst from Slurry Bubble Column Wax and Catalyst Recycle ", United States Patent 4,605,678, August 12, 1986.
2. Lorentzen, et al., "Solid/Liquid Slurry Treatment Apparatus and Catalytic Multi-phase Reactor ", United States Patent 5,520,890, May 28, 1996.
3. Jager, et al., "Process for Producing Liquid and Optionally Gaseous Products from Gaseous Reactants ", United States Patent 5,599,849, February 4, 1997.
4. Engel, et al. , "Method for Separating Liquid from a Slurry ", United States Patent 5,900,159, May 4, 1999.
5. Benham, et al., "Catalyst/Wax Separation Device for Slurry Fischer-Tropsch Reactor ", United States Patent 6,068,760, May 30, 2000.
6. Robert, et al., "Methods and Apparatus for Separating Fischer-Tropsch Catalysts from Liquid Hydrocarbon Product ", United States Patent 6,217,830, April 17, 2001.
7. B. H. Davis, "Technology Development for Iron and Cobalt Fischer-Tropsch Catalysts," Quarterly Report #8, DE-FC26-98FT40308, July - September, 2000.
8. B. H. Davis, "Technology Development for Iron and Cobalt Fischer-Tropsch Catalysts," Quarterly Report #9, DE-FC26-98FT40308, October - December, 2000.
9. B. H. Davis, "Technology Development for Iron and Cobalt Fischer-Tropsch Catalysts," Quarterly Report #10, DE-FC26-98FT40308, January - March, 2001.
10. Kirk-Othmer Encyclopedia of Chemical Technology (1993), volume 10, pages 841-847.
11. Shoemaker, W., "The Spectrum of Filter Media", ***A.I.Ch.E. Symposium Series***, 171, Vol. 73 (1977) 26-32.
12. Filtration Principles and Practices, Edited by Clyde Orr, Marcel Dekker, Inc. (1977).
13. Perry's Chemical Engineers' Handbook, 6th Edition, edited by D.W. Green, McGraw-Hill, Inc. (1984), pgs 5-42 to 5-43.

Table 1

Operating Conditions: SBCR and CSTR Comparison Experiments

	SBCR Run JKN-006 High Alpha	CSTR Run BAO-068 High Alpha
Catalyst	100Fe/5.1Si/2.0 Cu/5K	100Fe/5.1Si/2.0 Cu/5K
Initial Cat. loaded wt%	20	20
Catalyst. Activation:		
Gases	CO	CO
Gas space velocity (SL/hr-g Fe)	2.5	1.0
Temperature (^{o}C)	270	270
Pressure (atm.)	12	12
Synthesis Conditions:		
H_2/CO	0.7	0.7
Gas space velocity (SL/hr-g Fe)	5.0	4.6
Temperature (^{o}C)	270	270
Pressure (MPa)	1.21	1.21
Gas superficial velocity (cm/sec)	3	Stirred speed 750 RPM

Table 2. F-T Product Report CSTR/SBCR Comparison: High Alpha Catalyst			
Groups	**Range**	**CSTR wt% (2 samples)**	**SBCR wt% (3 samples)**
Light Gas	C_1	2.7 ± 0.2	1.8 ± 0.1
Gas	C_1 to C_4	14.0 ± 1.7	9.6 ± 0.1
Gasoline	C_5 to C_{11}	23.2 ± 2.6	20.6 ± 0.4
Diesel	C_{12} to C_{18}	15.4 ± 1.4	22.7 ± 2.3
Wax	C_{19} plus	44.6 ± 4.4	45.3 ± 2.8
	C_{12} plus	60.0 ± 3.0	68.0 ± 0.5
	C_5 plus	83.3 ± 1.9	88.6 ± 0.1

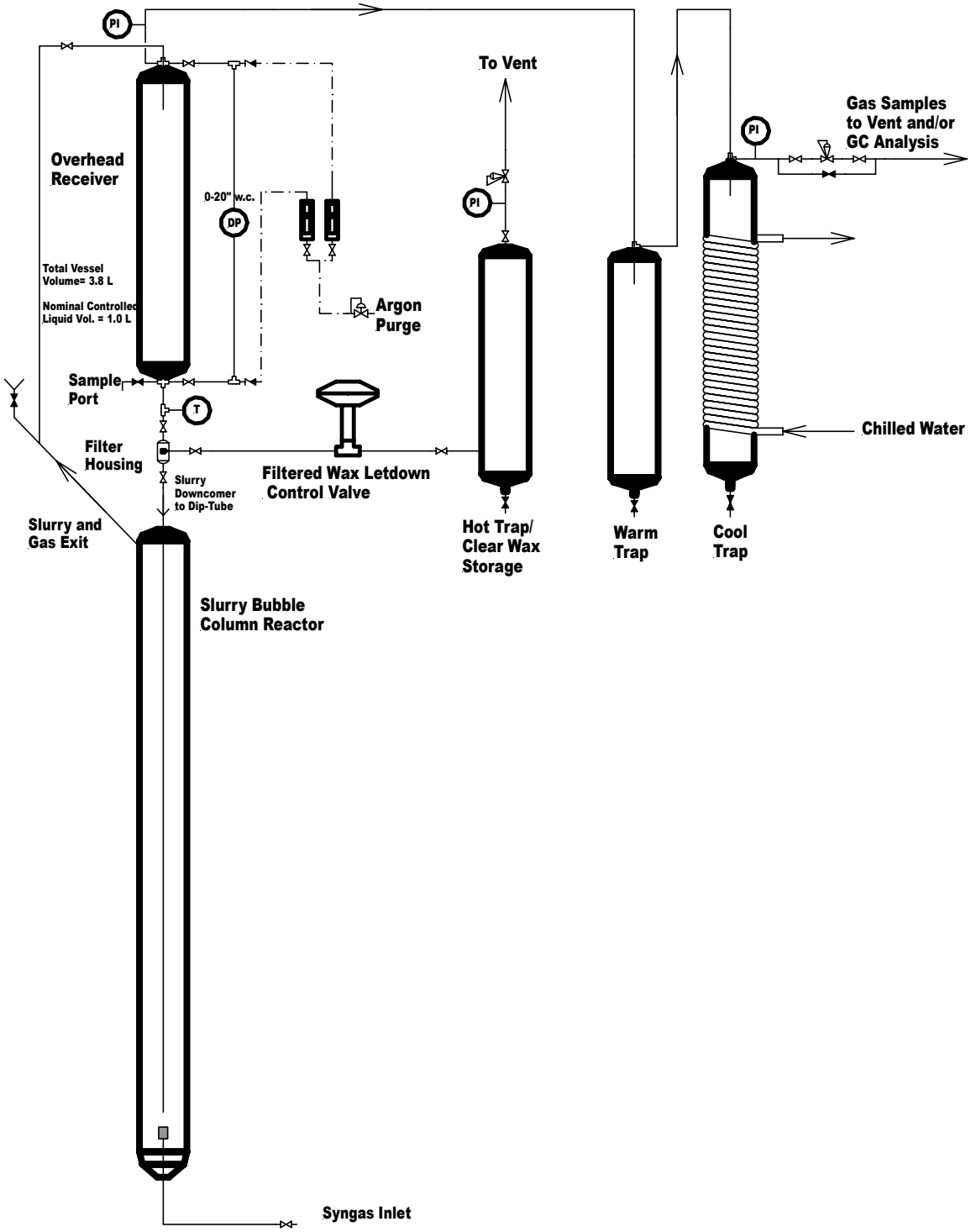

Figure 1. Schematic of the slurry bubble column reactor pilot plant.

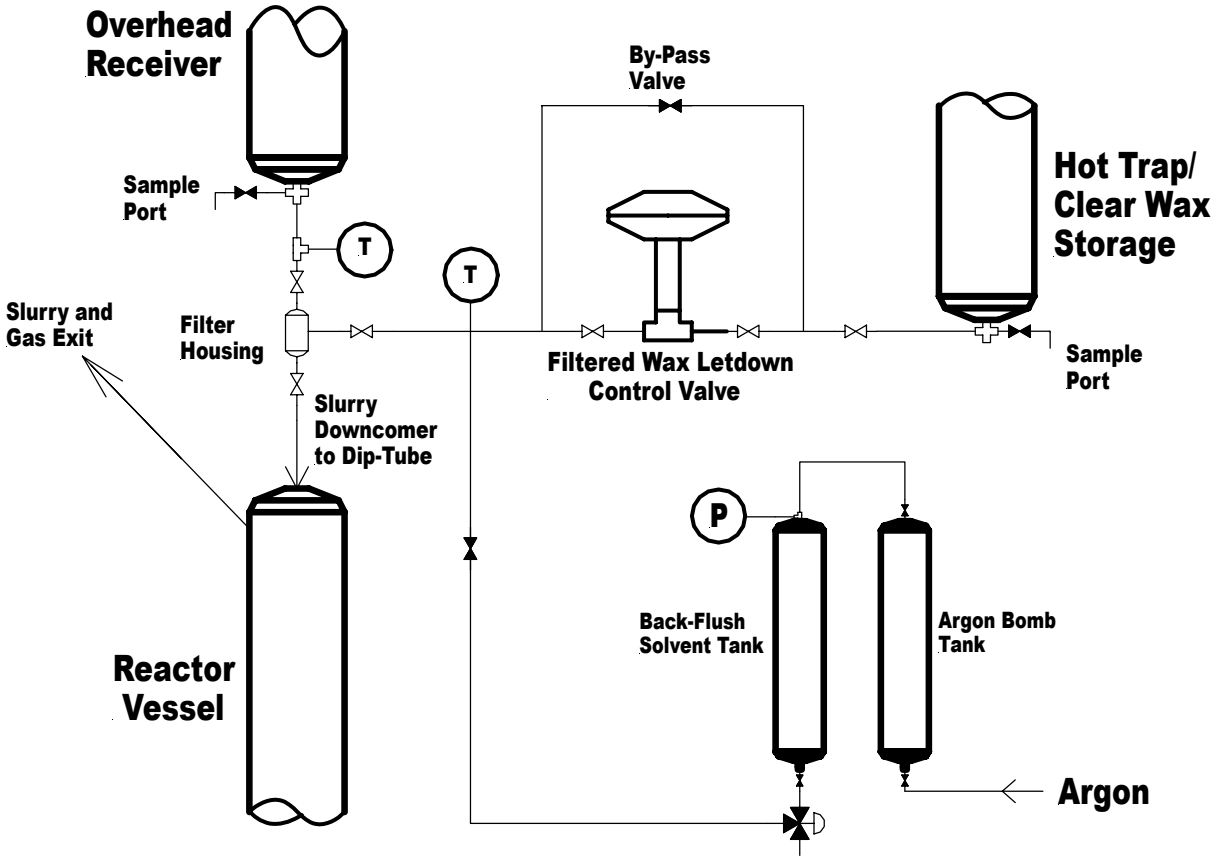

Figure 2. Detail schematic of the SBCR wax filtration and slurry level control systems.

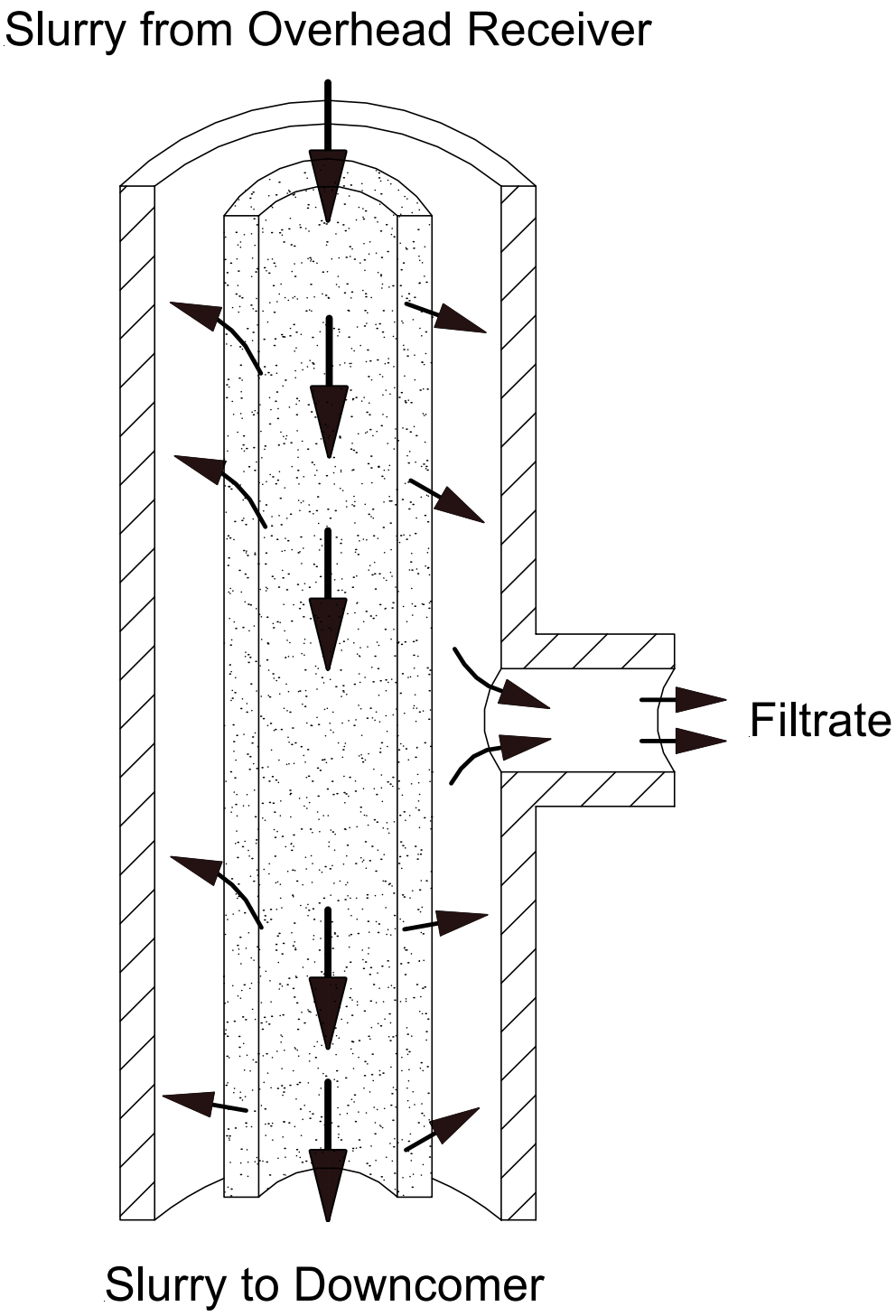

Figure 3. Cross-sectional depiction of the Mott cross-flow filter used in the SBCR filtration tests.

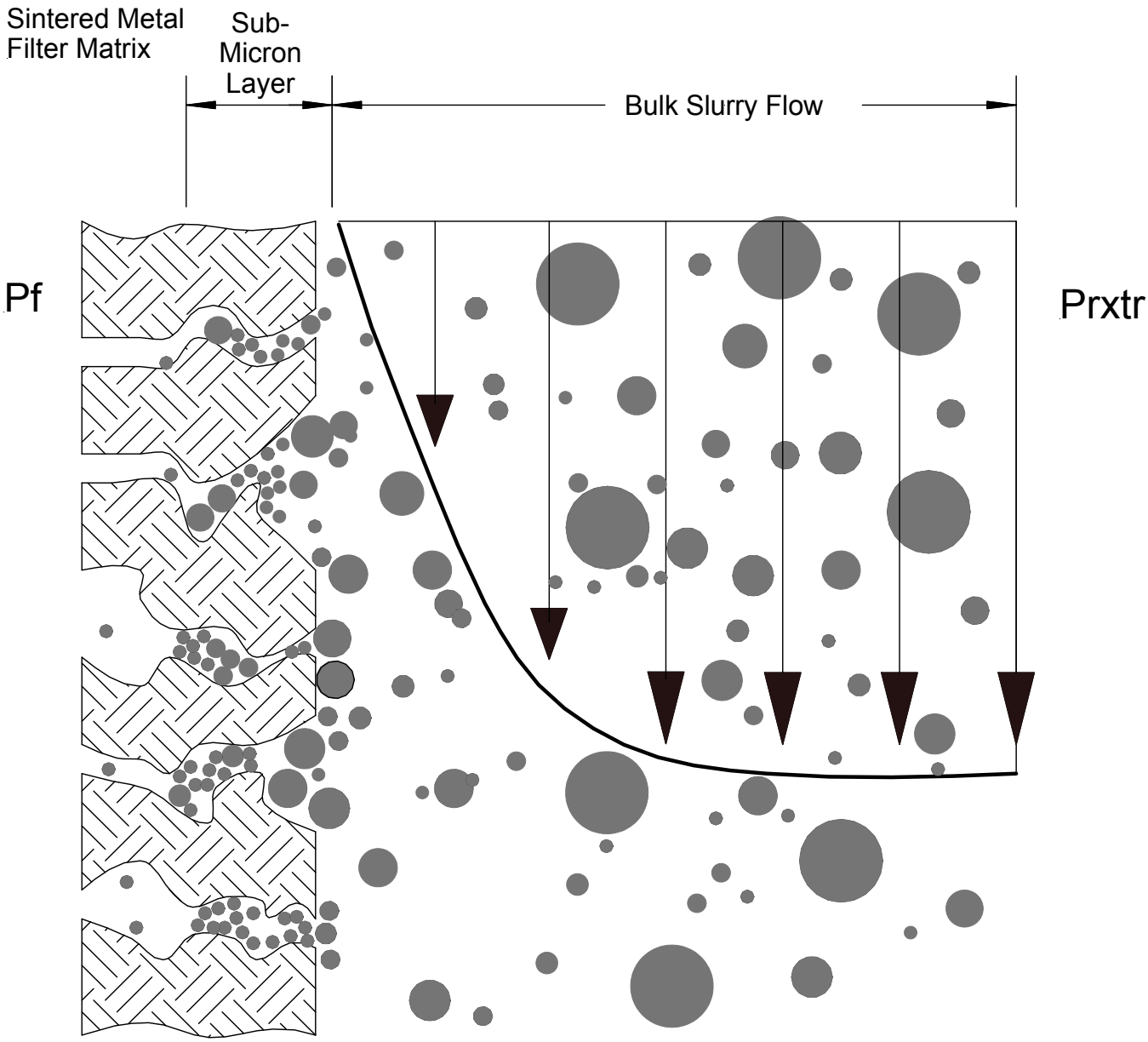

Figure 4. Illustration of the inertial filtration mechanism on the cross-flow filter media surface.

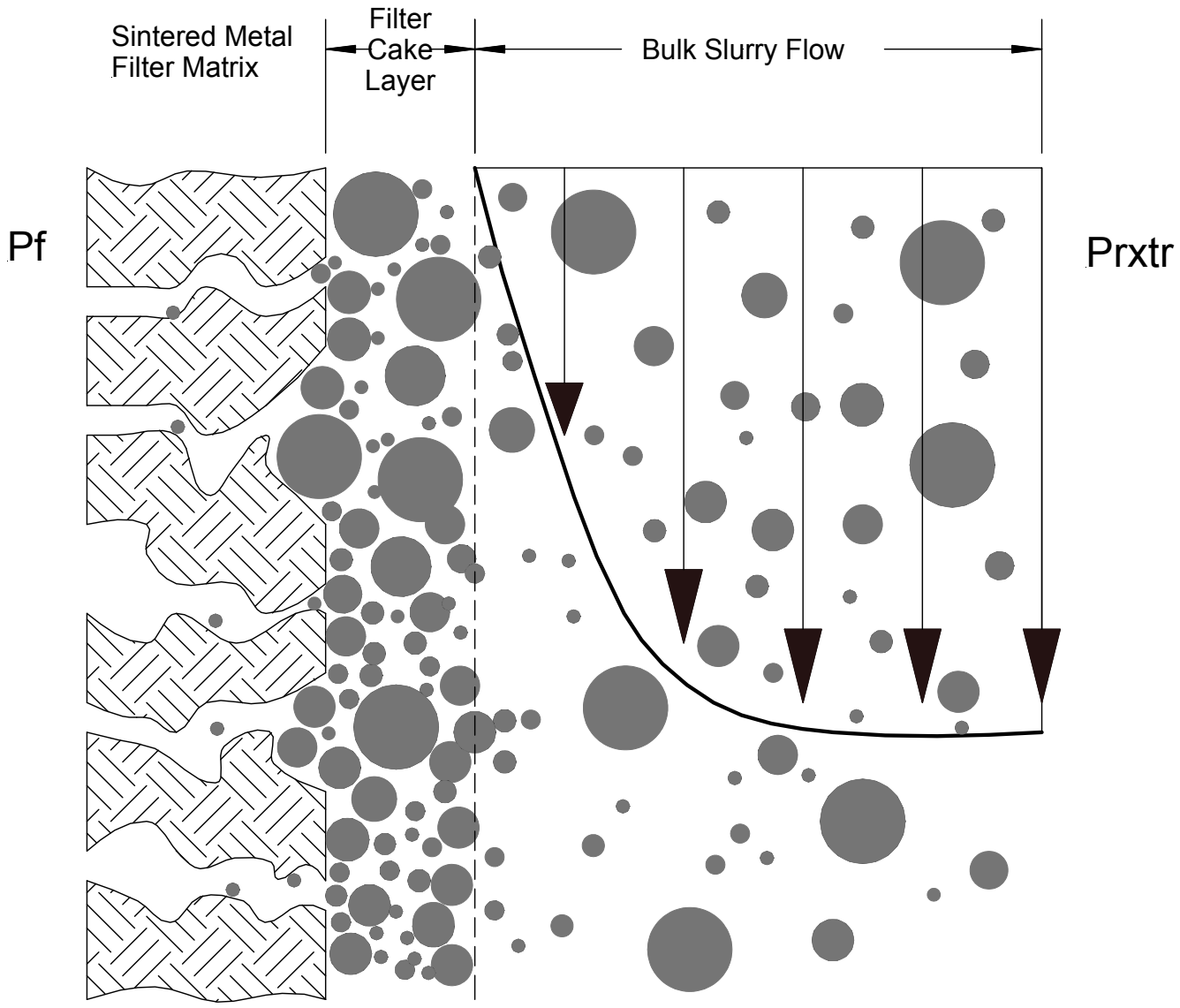

Figure 5. Illustration of the filter-cake mechanism on the cross-flow filter media surface.

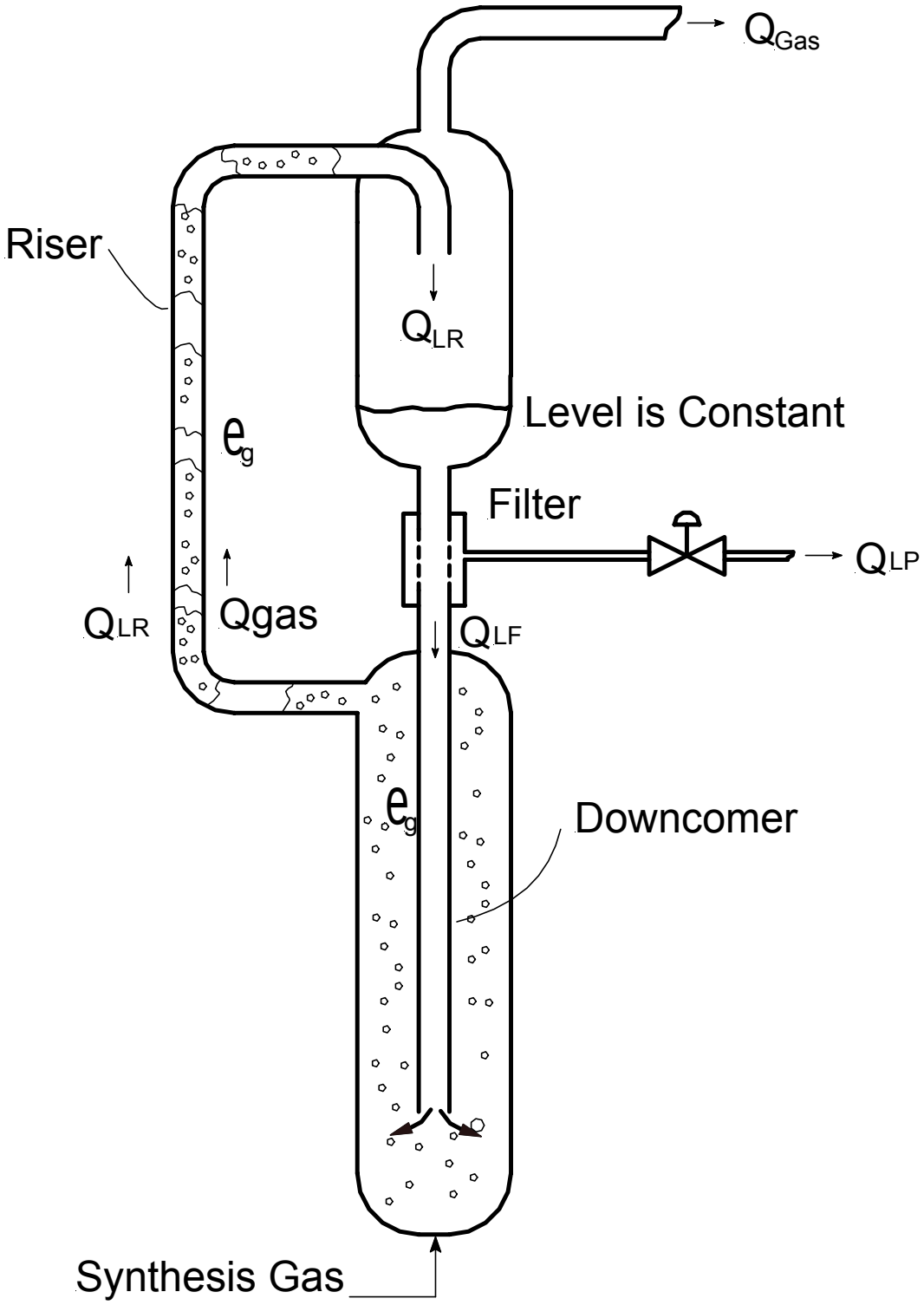

Figure 6. Simplified schematic of the SBCR recirculation flow circuit.

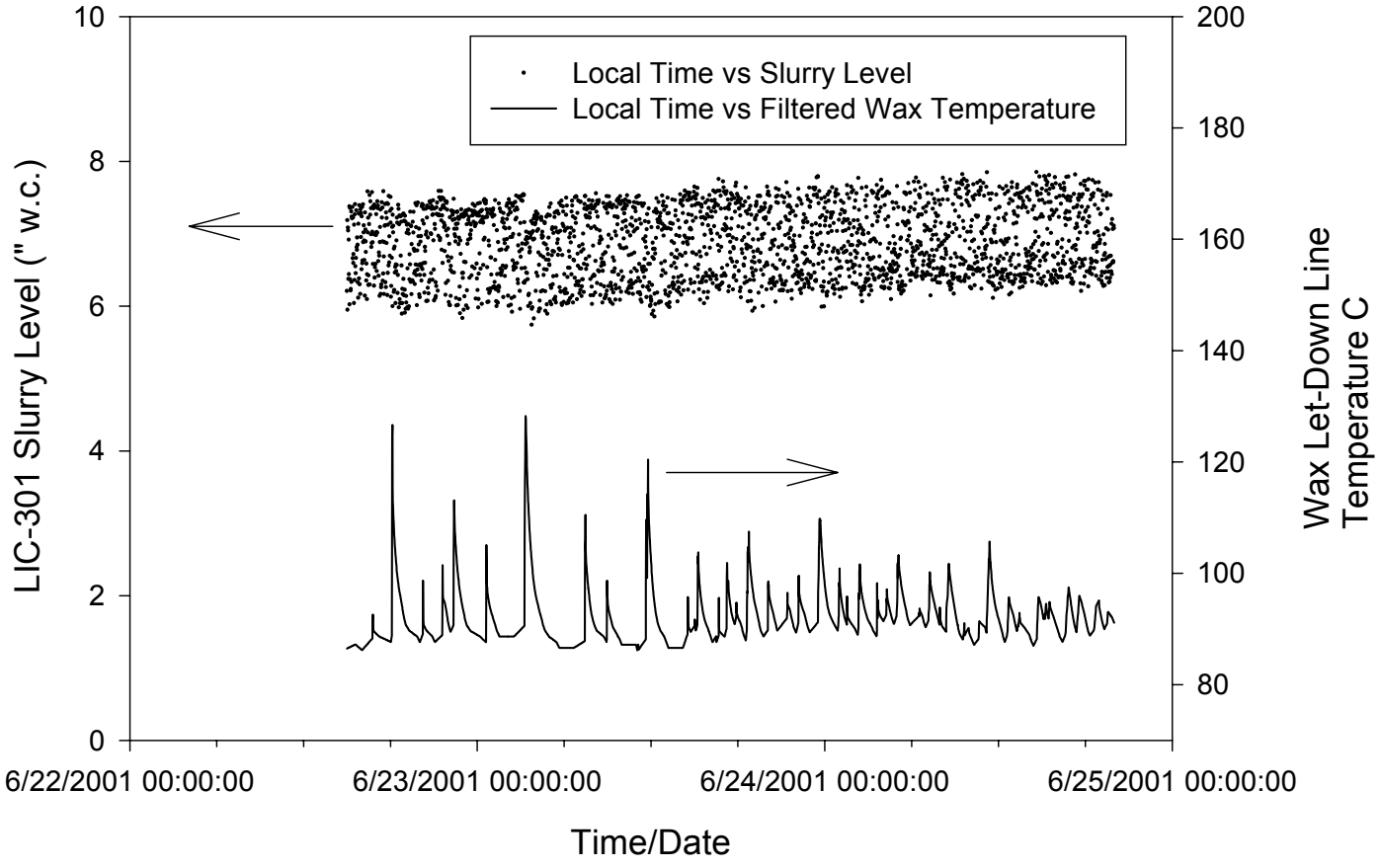

Figure 7. Plot of letdown filter line temperature and slurry level during the initial filtraiton cycles.

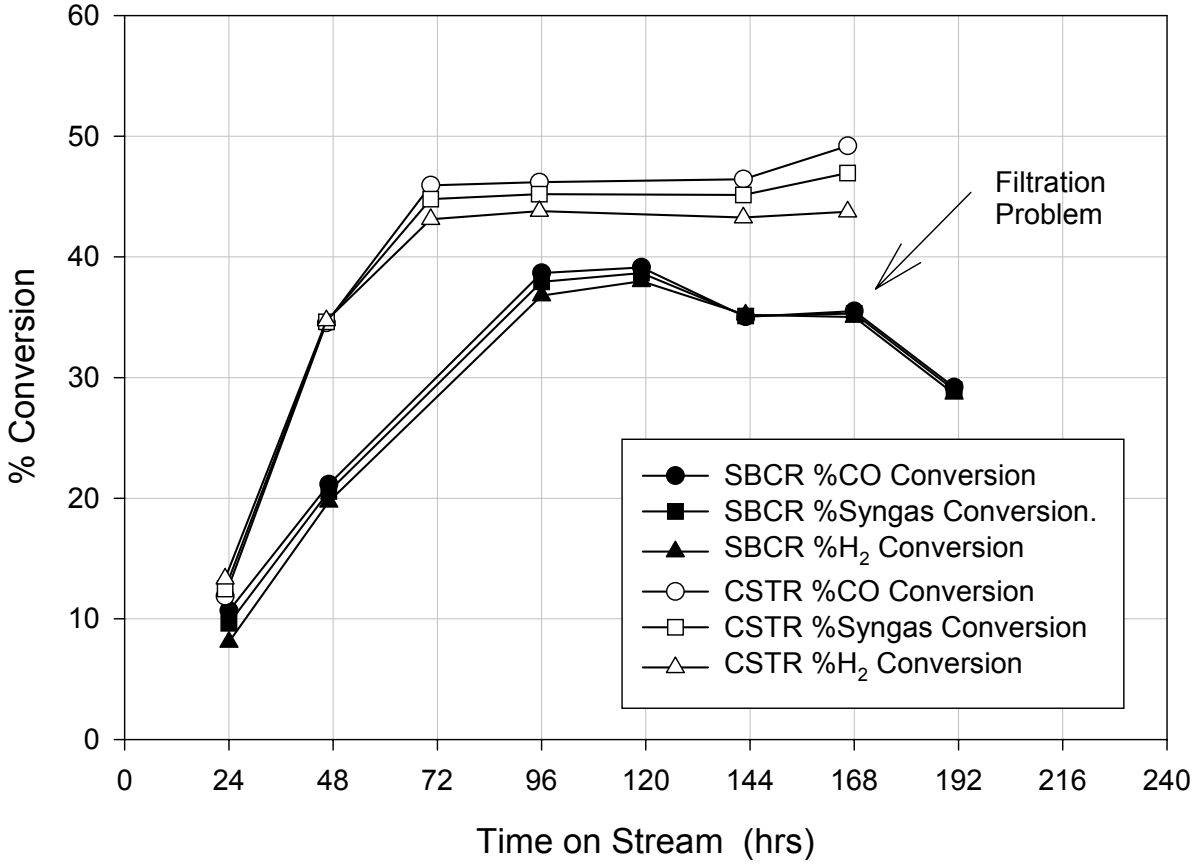

Figure 8. Gas conversion of SBCR and CSTR versus time-on-stream (starting conditions: T = 230ºC; P = 175 psig; H_2/CO ratio = 0.7; SV = 5.0 slph/g Fe; catalyst: RLS 100 Fe/5.1 Si/2.0 Cu/5K).

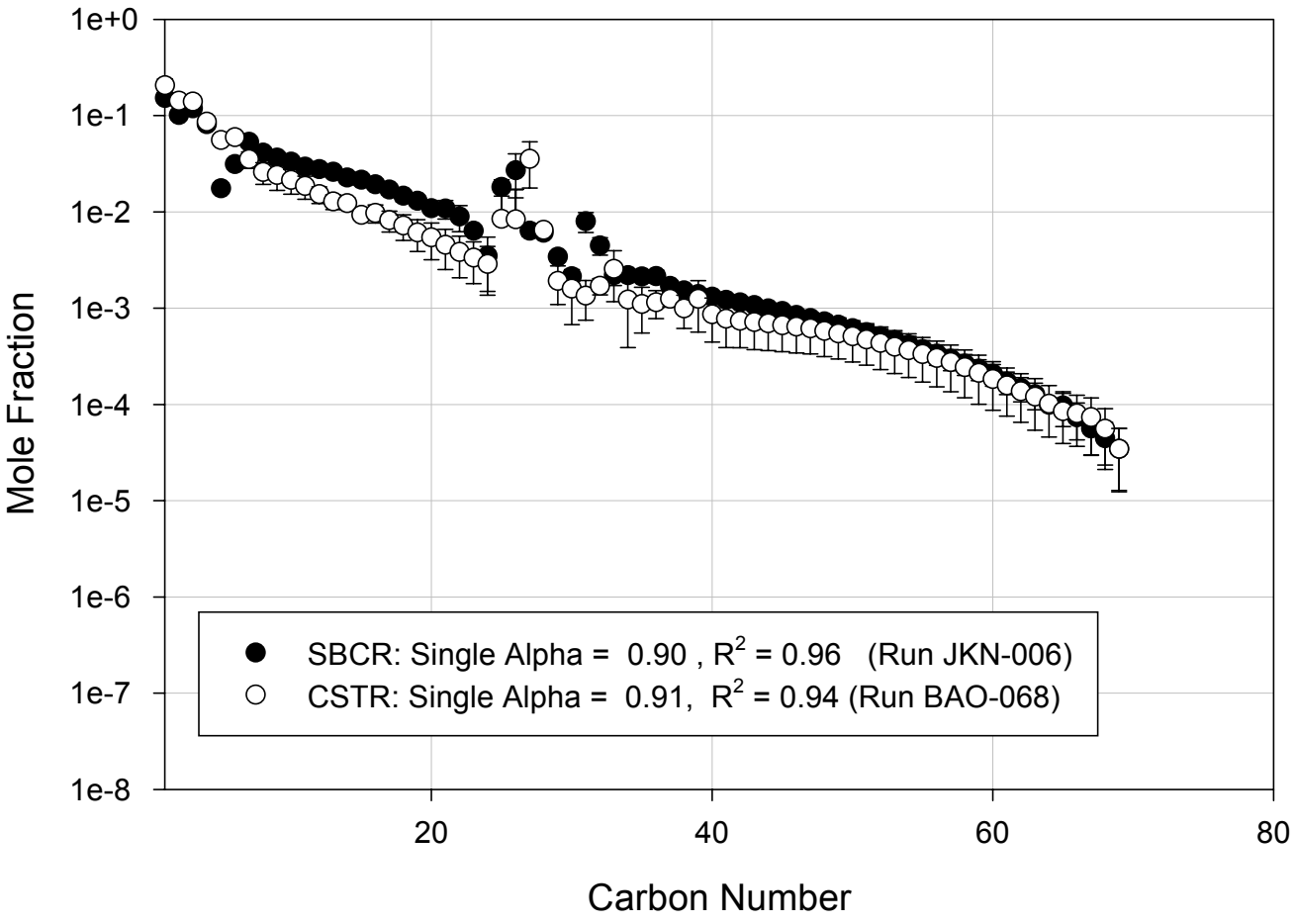

Figure 9. Alpha plot comparison between reactor types.

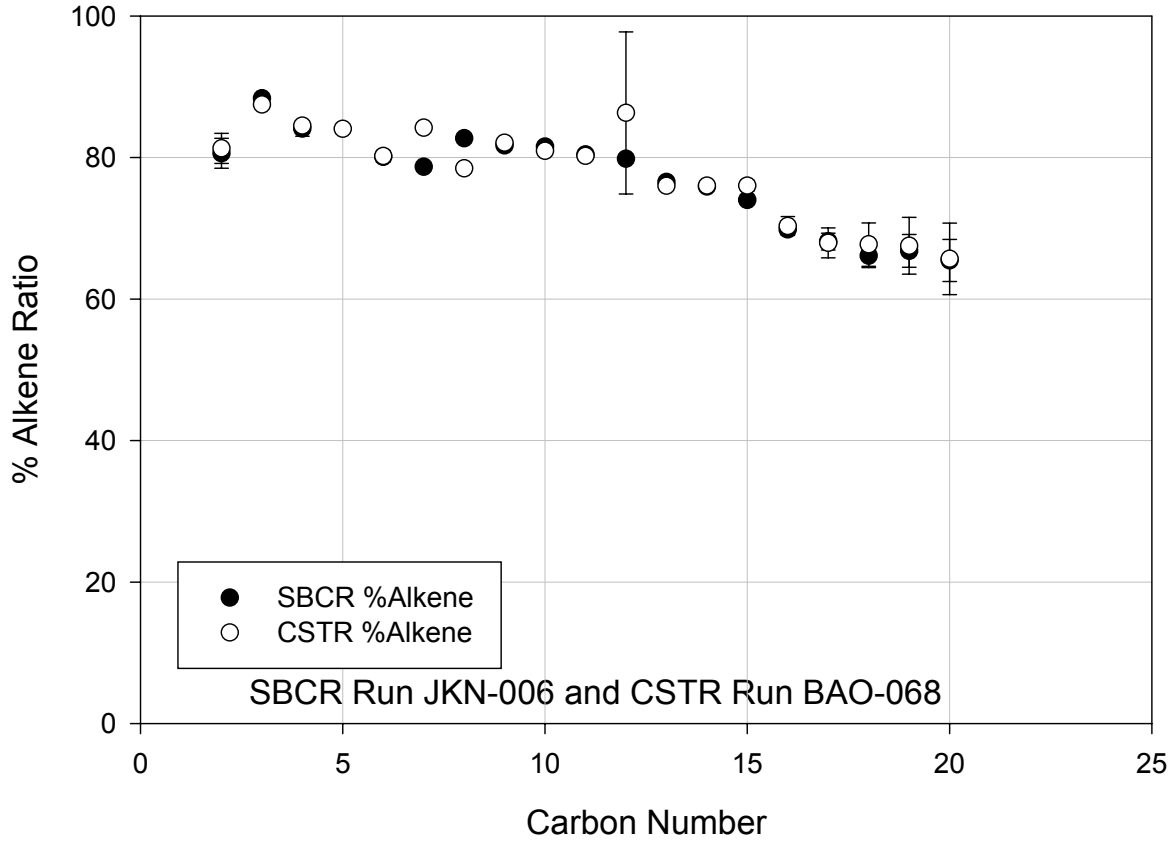

Figure 10. Alkene ratio comparison for SBCR and CSTR (SBCR run JKN-006 and CSTR run BAO-068).